Large angle πd scattering in the region of the (3,3) resonance

C. R. Ottermann, E. T. Boschitz, W. Gyles, W. List, and R. Tacik
Kernforschungszentrum Karlsruhe, Institut für Kernphysik und Institut für Experimentelle Kernphysik, der Universität Karlsruhe, D-7500 Karlsruhe, Federal Republic of Germany

R. R. Johnson and G. R. Smith
TRIUMF/University of British Columbia, Vancouver, British Columbia, Canada V6T 2A3

E. L. Mathie
University of Regina, Regina, Saskatchewan, Canada S4S 0A2
(Received 24 April 1985)

The differential cross section has been measured for the elastic πd scattering reaction between 73° and 172° at 11 energies between 124 and 324 MeV. The data agree well in the regions of angular overlap with previous measurements in the forward hemisphere, but disagree with some earlier large angle measurements. In particular, within the statistical accuracy of our data, no significant structure is observed in the energy dependence of the large angle cross sections.

I. INTRODUCTION

The interaction of pions with deuterons has been of interest for many years because of its fundamental importance for the understanding of pion interactions with complex nuclei.[1] In addition, the observations of resonance structures in spin dependent pp scattering above the threshold for pion production, and their interpretation as dibaryon resonances,[2] has stimulated experimental and theoretical work in the pionic reactions $\pi d \rightarrow \pi d$, $\pi d \rightarrow \pi NN$, $pp \rightarrow \pi d$, and $pp \rightarrow \pi NN$.[3]

Among these reactions, the πd elastic channel is by far the best studied case theoretically. Over a period of more than ten years many theoretical groups have refined their three-body Faddeev calculations to a high degree of sophistication.[4–10] In addition, there have been other theoretical approaches to describe πd scattering.[11–14] When compared with each other, and with experimental data, there is remarkable agreement between the predictions of the different groups for various observables, but only at forward angles ($\theta_\pi < 70°$). At larger angles this stability is lost, and the predicted observables depend sensitively on the fine details of the theory and/or the choice of the two-body input used.[15,16] It is this instability of the theory, or the uncertainty in the input, which prevents one at present from drawing conclusions about the possible existence of nonconventional dynamics from discrepancies with experimental data.

In comparison to the wealth of theoretical calculations, the body of experimental data in πd elastic scattering is still rather limited. Precise data on the differential cross section exist up to $\theta_{lab} = 130°$, at seven energies between $T_\pi = 80$ and 292 MeV.[17] Similarly accurate data have been measured over a narrower angular range at $T_\pi = 292$, 323, 417, and 476 MeV.[18] Unfortunately, the numerical values of these data are still unpublished. Earlier cross section data show inconsistencies or have large uncertainties.[19,20] At large angles (130° to 170°) there is one set of data at $T_\pi = 141$, 177, and 260 MeV, partly with large statistical and normalization errors.[21] Large angle data, some of which are remarkably inconsistent, also exist at energies above the (3,3) resonance.[22,23]

There have been recent measurements of the πd excitation function at 180° by three groups.[24–26] The cross sections of Refs. 25 and 26 differ by about a factor of 2. In these experiments, the observations of a structure are claimed around 225 MeV, and are taken as a possible indication for dibaryon resonances. Two comments are in order. In principle, large angle cross sections may be sensitive to dibaryon effects because the nonresonant background amplitudes (from conventional theory) are sufficiently small to allow for noticeable interference effects with resonant dibaryon amplitudes. However, the very smallness of the background amplitudes makes them quantitatively unreliable, particularly in view of the large theoretical uncertainties mentioned above. The second comment is in regard to the experimental techniques. The 180° scattering technique applied in both experiments requires an auxiliary magnet to be used between the π channel and the π spectrometer. The determination of the exact solid angle acceptence in this geometry is rather difficult. In the case of Ref. 25 this difficulty manifested itself in the measurement of πp cross sections at 180° which are at variance with most reliable phase shift analyses based on world data,[27] and also with recent experimental πp data.[28] Clearly it is important to measure cross sections not only at 180°, but also to extend them to an angular region where an overlap with the normal data taking setup can be achieved.

In view of this rather unsatisfactory experimental situation, it is the purpose of the present work to supplement the accurate data at forward angles[17] with equally precise data at large angles over a wide energy range. These cross section data, together with earlier extensive measurements of iT_{11} between 117 and 325 MeV,[29] and systematic measurements of tensor observables and spin transfer parame-

ters in the near future (SIN proposal R-82-12), will provide a sufficiently large data set to allow a meaningful phase shift analysis, and thus shed some light on the still open question of dibaryon signals in the πd elastic channel.

II. THE EXPERIMENT

The experiment was carried out in the $\pi M3$ area of the Swiss Institute of Nuclear Research (SIN). πd differential cross sections were measured by detecting the elastically scattered pions in coincidence with the recoil deuterons. Particle types were identified, and their energies measured, by recording both time of flight and pulse height information. πp differential cross sections were also measured at several energies with the same experimental apparatus, and compared with the data of Bussey *et al.*[30] This provided a check of the reliability and absolute normalization of the πd data.

The pion beam of the $\pi M3$ channel was focused on the scattering targets. At the beginning of the experiment the beam divergence and the beam profile at the target were studied with two multiwire proportional chambers (MWPC's). One was positioned at the target location, the other 1.4 m upstream from the target. The focusing and steering of the beam was optimized for all energies used in the experiment. Since the beam size at the target location was about 20×25 mm^2 FWHM, and varied with the pion momenta, a beam defining scintillation counter, $S1$ (10×15 mm^2 in area and 1 mm thick), was placed 10 cm in front of the target. A second beam defining scintillation counter, $S2$ (40×100 mm^2 in area and 2 mm thick), was positioned 1.5 m upstream from the target. During the experiment the MWPC at the target location was replaced by the scattering targets, while the other one was left in place to monitor the beam profile.

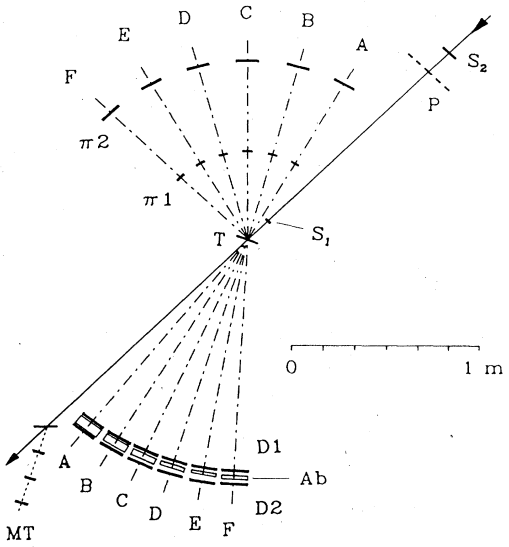

FIG. 1. Schematic drawing of the time of flight spectrometer, showing the incident pion counters ($S1$,$S2$), the beam profile chamber (P), an independent beam monitor telescope (MT), and the coincident pion and deuteron counter arrays ($\pi1$,$\pi2$,$D1$,$D2$). An absorber (Ab) was placed between $D1$ and $D2$ with thickness chosen to stop deuterons, thus discriminating against protons.

The detection system consisted of six pion scintillation counter telescopes at backward angles, and six associated deuteron scintillation counter telescopes at the corresponding forward angles. The experimental arrangement was essentially the same as that used in previous experiments,[29,31] see Fig. 1, except that the size of the deuteron counters was enlarged to 12.5×40 cm^2 in area in order to reduce the losses due to multiple scattering of low energy deuterons. This had been of less concern in previous experiments, which involved the determination of iT_{11}, and thus required only a measurement of relative cross sections. The angular acceptance of the pion telescopes was such that no particles scattered from counter $S1$ could be detected. The losses due to multiple scattering are discussed in more detail below.

The cross section was calculated from the expression

$$\frac{d\sigma}{d\Omega}=\frac{\text{YIELD}}{\text{BEAM}\times N_{\text{tgt}}\times\Delta\Omega\times\epsilon}$$

where YIELD defined the number of scattering events, BEAM the number of pions incident on the target, N_{tgt} the number of deuterons in the target per cm^2, $\Delta\Omega$ the effective solid angle (comprising the geometric solid angle along with pion decay and multiple scattering effects), and ϵ the combined efficiencies of the scintillation counters and the data acquisition system, which were typically 96% to 99%. BEAM was defined by the coincidence requirement $\text{BEAM}=\text{rf}\cdot S1\cdot\overline{S1}\cdot S2\cdot\overline{S2}$, where rf was the cyclotron radio frequency signal used for timing, and $\overline{S1}$ and $\overline{S2}$ were veto signals from upper level pulse height thresholds set on S1 and S2 to discriminate against protons from the $\pi M3$ channel. Most of these protons had already been eliminated by having their energy degraded before the last bending magnet of the $\pi M3$ beam line. A 5 mm carbon absorber was used for this purpose for energies below 275 MeV, 10 mm for higher energies. All electrons and most muons in the beam were rejected by the hardware time of flight coincidence between the beam defining counters and the rf signal. The remaining muon contamination of the beam was measured from the time of flight of the particles down the beamline. It varied between 1% (at higher energies) and 2% (at lower energies). A three counter monitor telescope (MT) 1.5 m downstream of the target was used to provide an independent measurement of the beam stability.

The beam momenta, including the effect of energy loss in the carbon absorber, were known from an earlier field chart of the first dipole magnet of the pion channel, which had been checked with particle range measurements.[32] The mean beam momentum is known to a precision of 0.4%. The momentum spread of the incoming beam was typically $\Delta P/P=\pm0.7\%$ for pions of about 300 MeV/c. At momenta $p<250$ MeV/c and $p>380$ MeV/c this was increased to $\pm1\%$ in order to raise the incident pion rate. The beam intensity (as defined by BEAM) was typically 10^6 pions per second.

For the measurement of the πd cross section CD_2 targets (0.227 g/cm^2 and 0.445 g/cm^2 thick) were used. For

the πp cross section the target was CH_2 (0.497 g/cm^2 thick). The isotopic purity of the targets was greater than 99%. The thickness is known to an accuracy of 1% for the 0.227 g/cm^2 CD_2 target, and to 2% for the others. The background from the quasifree πp reaction in carbon was explicitly measured with CH_2 and carbon targets. The thicknesses of these two background targets were chosen to match, in radiation length, the ones of the CD_2 and CH_2 targets, respectively, in order to keep the straggling effects the same.

The signature of a πd elastic scattering event was obtained from the difference in the deuteron and pion time-of-flight signals. The start signal (event trigger) for the CAMAC time-to-digital converters (TDC's) was the event coincidence BEAM$\cdot\pi 1\cdot\pi 2\cdot D1\cdot\overline{D2}$ with the rf signal in the BEAM coincidence determining the timing. $\pi 1\cdot\pi 2$ was the coincidence of the two counters in one of the pion detecting telescopes, while $D1\cdot\overline{D2}$ was the anticoincidence between the two counters in the corresponding deuteron detecting telescope. Absorbers were placed between the D1 and D2 counters in order to stop recoil deuterons after the D1 counters. The veto counters D2 rejected most protons coming from the scattering target. The analysis of the remaining ones is discussed below. For measurements of the πp scattering cross section the absorbers, as well as the anticoincidence requirement, were removed. The instrumental (timing) resolution was better than 0.5 ns, although kinematical broadening worsened this by a factor of 2 to 3.

A special electronic circuit was setup to measure the random events arising from the presence of multiple pions in each cyclotron beam burst. These were recorded on magnetic tape along with the foreground and background data, enabling correction of the data off line. The reliability of the circuit was tested by comparing the "random-corrected πd spectra" taken at different beam intensities between 4.0×10^5 pions per second and 2.1×10^6 pions per second. The corrected data were all consistent within a statistical uncertainty of 2%. At the beam rate used during the experiment the contribution due to random events amounted to 10%.

A typical raw random-corrected time-of-flight difference spectrum is shown in Fig. 2(a). The πd elastic peak on the left-hand side is clearly separated from the background events on the right-hand side. Of these, the ones with the shortest time of flight are a small fraction of the high energy protons from quasielastic πp reactions which were not rejected by the $D1\cdot\overline{D2}$ anticoincidence requirement due to geometrical and straggling effects. The remaining background events arise from lower energy protons from these reactions which stop in the $D1$ counter and are therefore also not vetoed. Figure 2(b) shows the corresponding random-corrected spectrum taken with a carbon target. Figure 2(c) shows the spectrum resulting from the subtraction of the "random-corrected carbon" from the "random-corrected CD_2 spectra." The remaining peak on the right-hand side in this spectrum is due to the πd$\rightarrow\pi$pn breakup reaction. The cross section for this reaction is strongly peaked at the kinematics corresponding to free πp$\rightarrow\pi$p. Therefore, as can be seen by inspection of the regions on either side of the πd elastic peak,

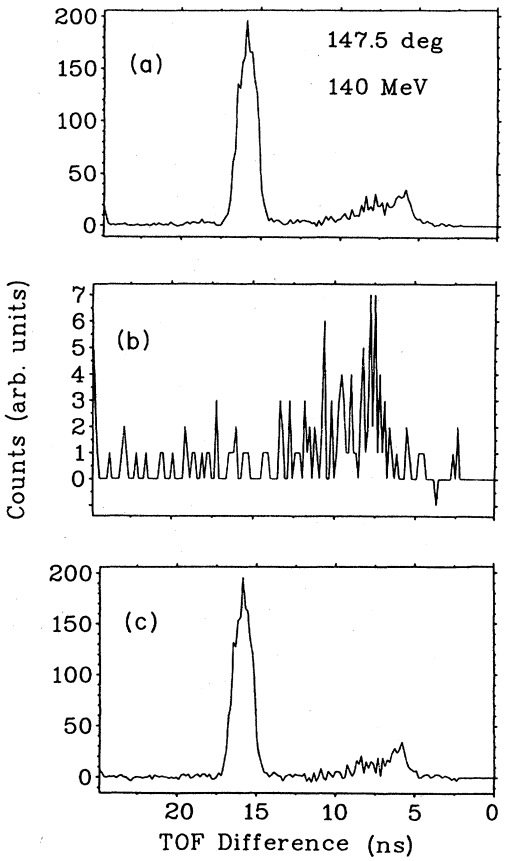

FIG. 2. Typical time of flight difference spectra obtained in the present experiment with (a) a CD_2 target, and (b) a carbon target. (c) is the result of subtracting (b) from (a). The peak on the left-hand side comes from πd elastic scattering; the bump on the right-hand side from the πd breakup reaction.

the background events do not extend there. Additional software cuts on individual TDC and analog-to-digital converter (ADC) spectra were thus found to be unnecessary. The yield of πd elastic scattering events was obtained by a straightforward integration of the πd peak. A similar procedure was followed for the πp elastic scattering measurement.

The geometric solid angle in this experiment was defined by the $\pi 2$ counters (10×30 cm^2 in area) situated 1.0 m from the scattering targets. The error in determining the solid angle due to possible misalignment of the detectors and fringe effects (pions hitting the scintillation counters at the edge) was estimated to be about 1%.

Uncertainties in the scattering angle θ_π, due to possible misalignment of the beam defining counters $S1$ and $S2$, the target, and the pion telescopes, were less than 0.3°. The angular acceptance due to the divergence of the incident pion beam and the dimensions of the $\pi 2$ detector was $\pm3°$.

III. CONSIDERATION OF CORRECTION FACTORS

Many factors which enter into the data analysis have been described so far. In addition, the following correc-

tions were applied to the data:

Pion decay losses, the detection of decay muons in the beam defining counters, and the influence of straggling effects on the beam definition were studied by means of a Monte Carlo simulation of the experimental setup. This resulted in a correction factor for BEAM of 2% for the lower pion energies and 1% for the higher ones.

With a similar Monte Carlo program the pion decay losses and the straggling effects of the scattered pions and the recoil deuterons in the targets, in air, and in the scintillation counters were investigated. Pions and muons could not be distinguished in the π detectors. Therefore, muons from decay in the forward direction did not affect the pion yield. As for π decays at larger angles, there was a nearly complete cancellation between events where a pion, initially traveling towards a pion counter, scattered or decayed and missed the counter, and events where a pion, initially missing the pion counter, scattered or decayed into it. For energies of $T_\pi > 140$ MeV the solid angle of the associated $D1$ counter was big enough not to affect this cancellation. The calculated correction factors varied from 1.01 for $T_\pi = 324$ MeV and $\theta_\pi = 140°$ to 1.12 for $T_\pi = 124$ MeV and $\theta_\pi = 105°$. The uncertainty of the corrections (1% to 2%) was added to the statistical error of the data points.

The attenuation of the number of incident pions due to absorption in the target was estimated from the πd and πC total absorption cross sections. The effects were found to be less than 0.4% in the worst case. Similarly, the absorption of the scattered pions in the material between the target center and the $\pi 2$ detector was estimated to be less than 0.8%, and the absorption of recoil deuterons was negligible.

Due to the large solid angle subtended by the $\pi 2$ detectors, a solid angle correction was applied using the angular dependence of the uncorrected data. The correction factor was 1.01 for $\theta_\pi = 170°$ and negligible for $\theta_\pi < 150°$.

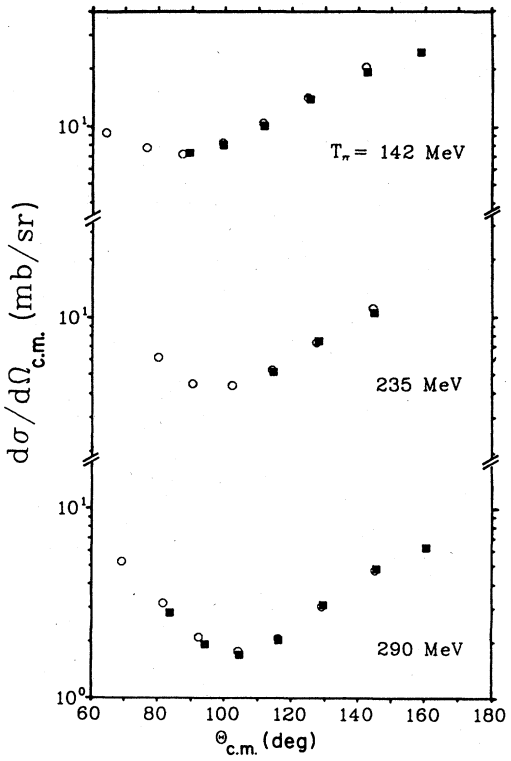

FIG. 3. Comparison of the πp data from this experiment (closed squares) with the results from Ref. 30 (open circles).

The linear addition of all the uncertainties arising from the factors discussed above resulted in an overall systematic uncertainty of 4% to 5% for the present data.

IV. RESULTS AND DISCUSSION

The πp cross sections obtained in this experiment are tabulated in Table I and displayed in Fig. 3 together with

TABLE I. The measured differential cross sections in πp elastic scattering.

	Laboratory system		c.m. system	
T_{lab}	Angle	$d\sigma/d\Omega$ (mb/sr)	Angle	$d\sigma/d\Omega$ (mb/sr)
142.1	75.0	8.03±0.34	89.2	7.42±0.31
	85.0	8.08±0.41	99.4	8.14±0.41
	97.5	9.10±0.37	111.6	10.23±0.42
	112.5	11.13±0.32	125.4	14.15±0.41
	132.5	13.42±0.40	142.5	19.61±0.59
	152.5	15.40±0.59	158.7	24.82±0.95
235.0	97.5	4.43±0.09	114.6	5.21±0.11
	112.5	5.56±0.11	128.0	7.58±0.15
	132.5	6.66±0.14	144.5	10.68±0.23
289.8	65.0	3.47±0.16	83.5	2.86±0.13
	75.0	2.10±0.08	94.2	1.95±0.08
	85.0	1.64±0.05	104.4	1.71±0.05
	97.5	1.73±0.03	116.2	2.09±0.03
	112.5	2.23±0.04	129.4	3.16±0.06
	132.5	2.90±0.05	145.5	4.90±0.09
	152.5	3.31±0.11	160.5	6.30±0.20

TABLE II. The measured differential cross sections in πd elastic scattering. The data marked by an asterisk are from earlier measurements presented in Fig. 2 of Ref. 31.

	Laboratory system		c.m. system	
T_{lab}	Angle	$d\sigma/d\Omega$ (mb/sr)	Angle	$d\sigma/d\Omega$ (mb/sr)
124.0	105.0	1.29 ±0.05	112.0	1.40 ±0.05
	110.0	1.40 ±0.05	116.8	1.54 ±0.06
	115.0	1.32 ±0.05	121.6	1.49 ±0.05
	120.0	1.33 ±0.05	126.2	1.53 ±0.06
	130.0	1.41 ±0.05	135.5	1.68 ±0.06
	140.0	1.38 ±0.05	144.6	1.70 ±0.07
	147.5	1.38 ±0.05	151.3	1.73 ±0.06
	155.0	1.50 ±0.06	158.0	1.91 ±0.07
	162.5	1.43 ±0.05	164.6	1.84 ±0.07
125.0(*)	90.0	1.13 ±0.09	97.4	1.14 ±0.09
	95.0	1.19 ±0.09	102.3	1.24 ±0.09
	100.0	1.18 ±0.09	107.2	1.25 ±0.09
	105.0	1.19 ±0.09	112.1	1.30 ±0.10
	110.0	1.21 ±0.09	116.8	1.35 ±0.10
	115.0	1.35 ±0.10	121.6	1.52 ±0.11
	120.0	1.44 ±0.11	126.3	1.65 ±0.13
	125.0	1.45 ±0.11	130.9	1.69 ±0.13
	130.0	1.40 ±0.11	135.5	1.67 ±0.13
	135.0	1.35 ±0.10	140.1	1.62 ±0.12
	140.0	1.34 ±0.10	144.6	1.64 ±0.12
133.0	95.0	1.22 ±0.05	102.5	1.27 ±0.05
	100.0	1.20 ±0.05	107.4	1.28 ±0.05
	105.0	1.24 ±0.05	112.2	1.34 ±0.05
	110.0	1.24 ±0.05	117.0	1.38 ±0.05
	115.0	1.28 ±0.05	121.7	1.45 ±0.06
	120.0	1.25 ±0.05	126.4	1.45 ±0.05
	130.0	1.23 ±0.05	135.6	1.47 ±0.06
	140.0	1.32 ±0.05	144.7	1.63 ±0.06
	147.5	1.32 ±0.05	151.4	1.66 ±0.07
	155.0	1.33 ±0.06	158.1	1.71 ±0.07
	162.5	1.36 ±0.06	164.7	1.77 ±0.08
	170.0	1.51 ±0.06	171.3	1.97 ±0.08
134.0(*)	85.0	1.13 ±0.09	92.6	1.12 ±0.09
	90.0	1.21 ±0.09	97.6	1.23 ±0.09
	95.0	1.23 ±0.09	102.5	1.29 ±0.09
	100.0	1.21 ±0.09	107.4	1.30 ±0.09
	105.0	1.19 ±0.09	112.2	1.31 ±0.10
	110.0	1.14 ±0.09	117.0	1.26 ±0.10
	115.0	1.33 ±0.09	121.8	1.50 ±0.10
	120.0	1.25 ±0.09	126.4	1.45 ±0.10
	125.0	1.36 ±0.09	131.1	1.60 ±0.10
	130.0	1.29 ±0.09	135.7	1.54 ±0.11
	135.0	1.31 ±0.10	140.2	1.59 ±0.12
	140.0	1.20 ±0.09	144.7	1.50 ±0.11
139.0	95.0	1.13 ±0.04	102.6	1.17 ±0.04
	105.0	1.18 ±0.04	112.4	1.28 ±0.04
	115.0	1.19 ±0.04	121.9	1.35 ±0.04
	130.0	1.14 ±0.04	135.7	1.37 ±0.05
	147.5	1.17 ±0.04	151.5	1.48 ±0.05
	162.5	1.16 ±0.05	164.7	1.51 ±0.06
140.0(*)	85.0	1.19 ±0.09	92.7	1.19 ±0.09
	90.0	1.25 ±0.09	97.7	1.27 ±0.09

TABLE II. (*Continued*).

	Laboratory system		c.m. system	
T_{lab}	Angle	$d\sigma/d\Omega$ (mb/sr)	Angle	$d\sigma/d\Omega$ (mb/sr)
	95.0	1.18 ±0.09	102.7	1.22 ±0.09
	100.0	1.10 ±0.09	107.6	1.17 ±0.09
	105.0	1.17 ±0.09	112.4	1.27 ±0.10
	110.0	1.12 ±0.09	117.2	1.24 ±0.10
	115.0	1.21 ±0.09	121.9	1.39 ±0.10
	120.0	1.14 ±0.09	126.5	1.33 ±0.10
	125.0	1.23 ±0.09	131.2	1.46 ±0.10
	130.0	1.17 ±0.09	135.8	1.41 ±0.10
	135.0	1.15 ±0.09	140.3	1.41 ±0.11
	140.0	1.13 ±0.09	144.8	1.41 ±0.11
146.0(*)	85.0	1.17 ±0.09	92.9	1.16 ±0.09
	90.0	1.17 ±0.09	97.9	1.19 ±0.09
	95.0	1.11 ±0.09	102.8	1.15 ±0.09
	100.0	1.10 ±0.09	107.7	1.17 ±0.09
	105.0	1.03 ±0.09	112.5	1.12 ±0.09
	110.0	1.04 ±0.09	117.3	1.16 ±0.10
	115.0	1.13 ±0.09	122.0	1.29 ±0.10
	120.0	1.09 ±0.09	126.7	1.27 ±0.10
	125.0	1.09 ±0.09	131.3	1.30 ±0.10
	130.0	1.11 ±0.09	135.8	1.35 ±0.11
	135.0	1.04 ±0.09	140.4	1.29 ±0.11
	140.0	1.01 ±0.08	144.9	1.25 ±0.09
151.0(*)	85.0	1.09 ±0.09	93.0	1.08 ±0.09
	90.0	1.08 ±0.09	98.0	1.10 ±0.09
	95.0	1.04 ±0.09	102.9	1.08 ±0.09
	100.0	1.09 ±0.09	107.8	1.16 ±0.09
	105.0	0.98 ±0.09	112.6	1.07 ±0.09
	110.0	0.96 ±0.08	117.4	1.07 ±0.09
	115.0	1.04 ±0.09	122.1	1.18 ±0.10
	125.0	1.02 ±0.09	131.4	1.20 ±0.10
	130.0	1.02 ±0.09	135.9	1.23 ±0.10
	135.0	0.92 ±0.08	140.5	1.13 ±0.09
	140.0	0.91 ±0.07	144.9	1.14 ±0.08
178.8	95.0	0.580±0.019	103.5	0.607±0.020
	105.0	0.571±0.019	113.2	0.629±0.021
	115.0	0.527±0.019	122.6	0.609±0.022
	130.0	0.446±0.016	136.4	0.550±0.020
	140.0	0.398±0.016	145.3	0.507±0.021
	147.5	0.393±0.017	151.9	0.512±0.022
	155.0	0.386±0.017	158.5	0.511±0.023
	162.5	0.400±0.017	165.0	0.536±0.023
	170.0	0.396±0.017	171.4	0.535±0.023
200.8	95.0	0.336±0.012	104.0	0.354±0.013
	105.0	0.295±0.011	113.7	0.328±0.012
	115.0	0.281±0.011	123.0	0.327±0.012
	130.0	0.253±0.010	136.7	0.316±0.012
	140.0	0.240±0.011	145.6	0.310±0.014
	147.5	0.209±0.009	152.2	0.277±0.012
	155.0	0.227±0.011	158.6	0.305±0.015
	170.0	0.245±0.012	171.5	0.337±0.017
217.8	100.0	0.194±0.005	109.2	0.210±0.005
	110.0	0.186±0.005	118.7	0.214±0.005
	120.0	0.172±0.004	128.0	0.207±0.005

TABLE II. (*Continued*).

	Laboratory system		c.m. system	
T_{lab}	Angle	$d\sigma/d\Omega$ (mb/sr)	Angle	$d\sigma/d\Omega$ (mb/sr)
	130.0	0.160±0.004	137.0	0.202±0.004
	135.0	0.164±0.005	141.4	0.211±0.006
	140.0	0.165±0.006	145.8	0.216±0.007
	145.0	0.161±0.004	150.2	0.214±0.005
	150.0	0.168±0.007	154.5	0.227±0.009
	155.0	0.167±0.006	158.8	0.228±0.008
	160.0	0.179±0.004	163.1	0.246±0.006
	165.0	0.164±0.007	167.3	0.228±0.010
227.9	85.0	0.175±0.006	94.7	0.174±0.006
	95.0	0.162±0.006	104.6	0.172±0.006
	105.0	0.148±0.006	114.2	0.166±0.006
	115.0	0.132±0.005	123.5	0.155±0.006
	125.0	0.139±0.005	132.6	0.172±0.006
	135.0	0.136±0.005	141.5	0.176±0.007
	145.0	0.142±0.006	150.3	0.190±0.008
	155.0	0.139±0.006	158.9	0.191±0.008
	165.0	0.148±0.006	167.4	0.207±0.009
254.5	120.0	0.075±0.004	128.6	0.092±0.004
	130.0	0.077±0.004	137.5	0.099±0.005
	135.0	0.089±0.004	141.9	0.117±0.005
	140.0	0.090±0.005	146.3	0.121±0.006
	147.5	0.099±0.005	152.7	0.135±0.007
	155.0	0.107±0.004	159.1	0.150±0.005
	162.5	0.120±0.006	165.4	0.171±0.008
	170.0	0.120±0.007	171.7	0.172±0.010
256.0(*)	80.0	0.107±0.014	90.3	0.104±0.013
	90.0	0.075±0.006	100.3	0.077±0.007
	100.0	0.061±0.005	110.0	0.067±0.006
	110.0	0.071±0.004	119.4	0.082±0.005
	120.0	0.070±0.004	128.6	0.086±0.005
	130.0	0.084±0.005	137.5	0.108±0.007
273.5	72.5	0.113±0.004	82.9	0.104±0.004
	82.5	0.057±0.003	93.2	0.056±0.002
	92.5	0.044±0.002	103.1	0.047±0.002
	102.5	0.046±0.002	112.7	0.052±0.002
	112.5	0.051±0.002	122.1	0.061±0.003
	132.5	0.066±0.003	140.0	0.086±0.004
	142.5	0.076±0.003	148.6	0.103±0.004
	152.5	0.087±0.005	157.1	0.122±0.007
	162.5	0.098±0.004	165.5	0.142±0.006
	170.0	0.104±0.005	171.7	0.151±0.007
275.0(*)	65.0	0.223±0.025	75.0	0.196±0.022
	85.0	0.048±0.005	95.7	0.048±0.005
	95.0	0.042±0.003	105.6	0.045±0.003
	100.0	0.044±0.003	110.4	0.048±0.004
	105.0	0.042±0.003	115.1	0.048±0.004
	110.0	0.045±0.003	119.8	0.054±0.004
	120.0	0.059±0.004	128.9	0.073±0.005
	130.0	0.065±0.004	137.8	0.084±0.006
	140.0	0.073±0.004	146.5	0.099±0.006
292.5	95.0	0.027±0.002	105.9	0.029±0.002
	105.0	0.032±0.002	115.5	0.037±0.002
	115.0	0.038±0.002	124.7	0.046±0.003

TABLE II. (*Continued*).

	Laboratory system		c.m. system	
T_{lab}	Angle	$d\sigma/d\Omega$ (mb/sr)	Angle	$d\sigma/d\Omega$ (mb/sr)
	130.0	0.053±0.002	138.1	0.069±0.003
	140.0	0.062±0.003	146.7	0.085±0.004
	147.5	0.065±0.002	153.1	0.092±0.003
	155.0	0.072±0.003	159.4	0.104±0.004
	162.5	0.083±0.003	165.6	0.121±0.004
	170.0	0.091±0.004	171.8	0.135±0.006
294.0(*)	67.5	0.121±0.018	78.1	0.108±0.016
	75.0	0.064±0.007	85.9	0.060±0.007
	82.5	0.032±0.003	93.6	0.031±0.003
	90.0	0.025±0.002	101.1	0.026±0.002
	97.5	0.028±0.002	108.4	0.030±0.002
	105.0	0.032±0.002	115.5	0.037±0.003
	112.5	0.036±0.003	122.4	0.043±0.004
	120.0	0.041±0.003	129.2	0.052±0.004
	127.5	0.046±0.003	135.9	0.061±0.004
	135.0	0.055±0.004	142.4	0.073±0.006
323.5	95.0	0.018±0.001	106.5	0.019±0.001
	100.0	0.020±0.002	111.3	0.023±0.003
	105.0	0.020±0.001	116.0	0.023±0.002
	110.0	0.022±0.002	120.7	0.026±0.003
	115.0	0.028±0.002	125.2	0.034±0.002
	120.0	0.033±0.003	129.7	0.042±0.004
	130.0	0.041±0.002	138.5	0.054±0.003
	140.0	0.047±0.002	147.0	0.065±0.003
	147.5	0.055±0.002	153.4	0.079±0.003
	155.0	0.059±0.003	159.6	0.087±0.004
	162.5	0.065±0.003	165.7	0.096±0.004
	170.0	0.073±0.003	171.9	0.110±0.005

cross sections from Ref. 30, which are generally considered the most precise πp data available in this energy range.[33] There is good agreement within the uncertainties of the data from both experiments. This indicates that pion decay and multiple scattering corrections, which are comparable in the πp and πd scattering, have been treated correctly.

The measured πd cross sections are listed in Table II. Also included are the numerical values of the cross section shown in an earlier publication.[31] The two data sets are plotted together at several energies in Fig. 4. Although the same technique was employed, the earlier experiment was performed with different targets and detectors, and thus constitutes an essentially independent measurement. The evident agreement between the two results is therefore gratifying. Note that the larger error bars on the data from Ref. 31 result partly from larger uncertainties in the multiple scattering losses due to the smaller size of the recoil deuteron counters used.

The present data is shown in Figs. 5(a) and (b) together with the differential cross sections from Refs. 17, 18, 20, and 21. In general, there is good agreement in the region of the angular overlap between the different experiments. This is not true for the data of Ref. 21 at 179 MeV, and for that of Ref. 20 at 228 MeV. Note that the uncertain-

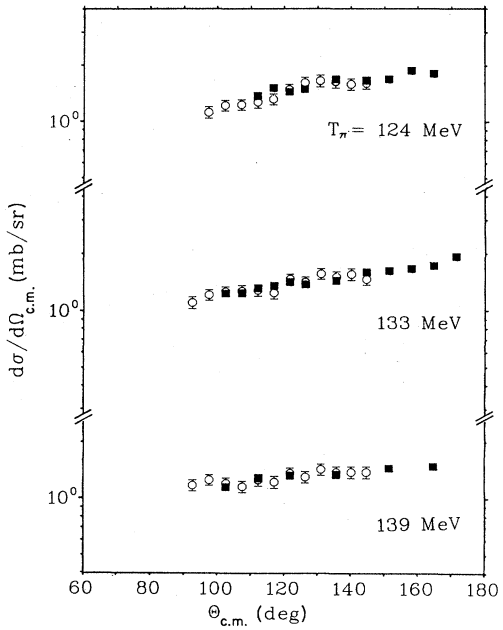

FIG. 4. Comparison of the πd data from this experiment (closed squares) with previous ones reported in Ref. 31 (open circles).

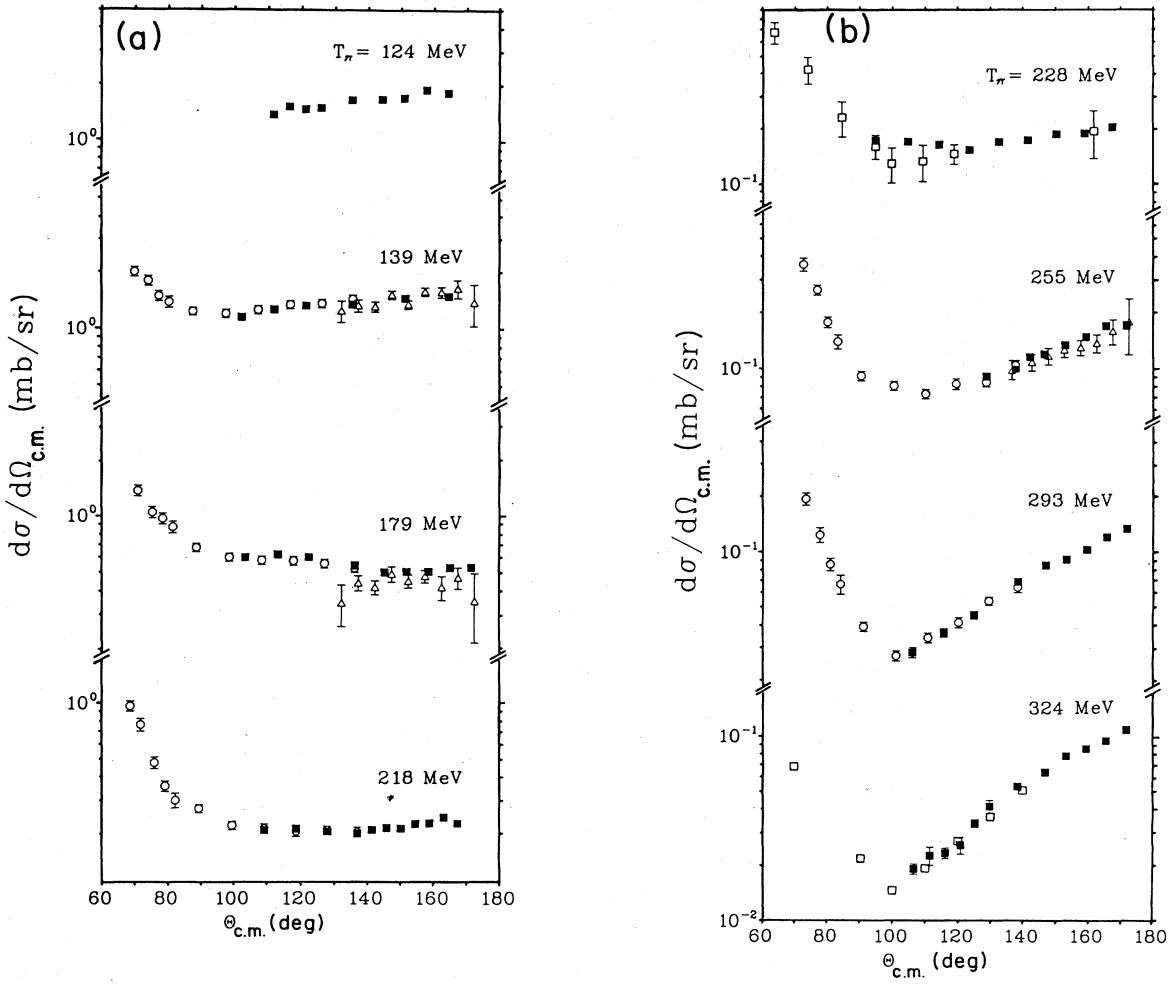

FIG. 5. (a) Comparison of the present data (closed squares) with those from Ref. 17 (open circles), and Ref. 21 (open triangles). (b) Comparison of the present data (closed squares) with those from Ref. 17 (open circles), Refs. 18 and 20 (open squares), and Ref. 21 (open triangles).

TABLE III. Values for the πd elastic differential cross sections at 180°, extrapolated from a linear fit to the measured data.

	Laboratory system		c.m. system	
T_{lab}	Angle	$d\sigma/d\Omega$ (mb/sr)	Angle	$d\sigma/d\Omega$ (mb/sr)
124.0	180.0	1.49 ±0.05	180.0	1.94 ±0.06
133.0		1.38 ±0.05		1.81 ±0.07
139.0		1.17 ±0.04		1.54 ±0.06
178.8		0.40 ±0.02		0.54 ±0.03
200.8		0.227±0.006		0.315±0.008
217.8		0.180±0.005		0.253±0.008
227.9		0.149±0.006		0.210±0.009
254.5		0.133±0.005		0.192±0.006
273.5		0.115±0.004		0.167±0.006
292.5		0.098±0.003		0.145±0.004
323.5		0.079±0.004		0.119±0.006

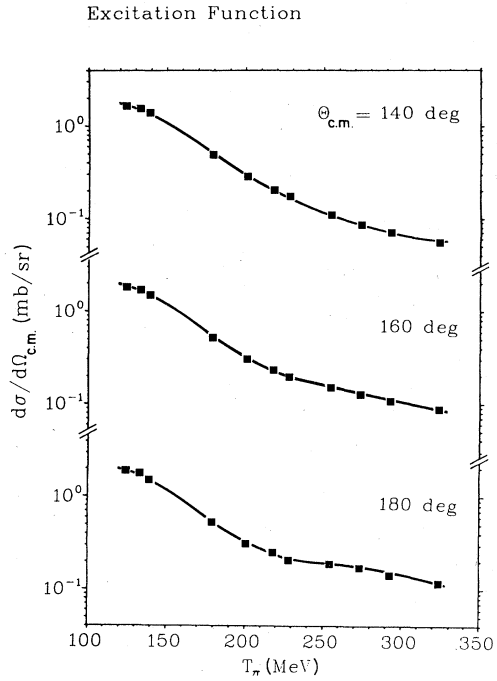

FIG. 6. Energy dependence of the πd cross section at $\theta_\pi^{c.m.} = 140°$, 160°, and 180°. The points at 140° and 160° are interpolated, while the ones at 180° are extrapolated from the present data. The curves are meant to guide the eye.

ties of the present data are a significant improvement over the previously existing data.

In regard to the question of structures in the energy dependence of large angle πd scattering, the angular distributions of the measured cross sections have been fitted in order to interpolate the data to 140° and 160° c.m., and extrapolate them to 180° c.m. (values presented in Table III). The energy dependence of the cross sections at these three angles is shown in Fig. 6. A line to guide the eye has been drawn through the data points. This line serves to illustrate the relative smoothness of the excitation functions. In contrast to the claims of Refs. 25 and 26, no pronounced structure is observed in the extrapolated data

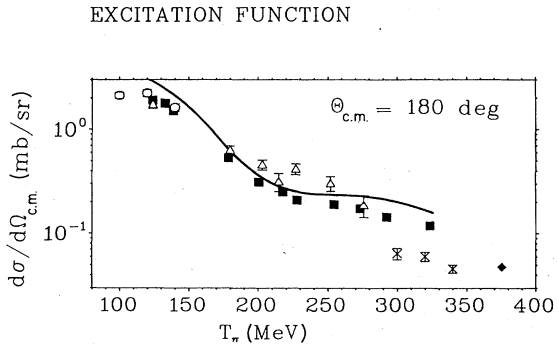

FIG. 7. Energy dependence of the πd cross section at $\theta_\pi^{c.m.} = 180°$ extrapolated from the present data (closed squares), along with the data of Ref. 24 (open circles), Ref. 25 (open triangles), and Ref. 23 (crosses). Also included is a higher energy π^-d point from Ref. 22 (closed diamond). The curve represents the calculation of Garcilazo (Ref. 34).

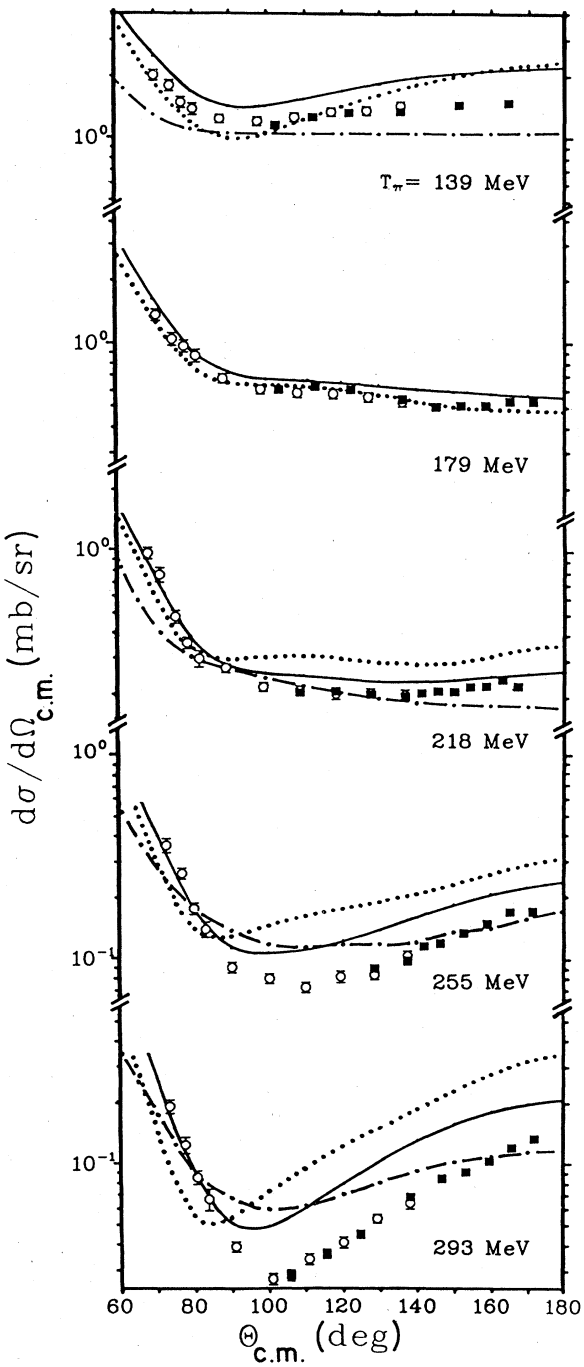

FIG. 8. Comparison of our data (closed squares) and those of Ref. 17 (open circles) with theoretical predictions from Garcilazo (Ref. 34) (solid line), Fayard *et al.* (Refs. 15 and 35) (dotted line), and Pöpping (Ref. 14) (dot-dashed line), at several energies.

at 180°, which are illustrated again, on a larger scale, in Fig. 7. One does note a minor change in the slope of the data at around 230 MeV. However, this change is predicted by the calculation of Garcilazo,[34] which does not include any exotic dibaryon effects.

Predictions for πd differential cross sections from Garcilazo,[34] Fayard *et al.*,[15,35] and Pöpping,[14] which represent only a few of the many existing theoretical calculations, are shown along with the present large angle data, and the small angle data of Ref. 17, at five energies in Fig. 8. The former two calculations are based on a three-body Faddeev approach, while the latter employs a two-nucleon force model with Δ isobar and π degrees of freedom. The results of the two Faddeev calculations, although differing in detail (treatment of absorption, off-shell effects, and the use of a relativistic spin formalism), share two general features: they are in fairly good agreement with the experimental data in the forward hemisphere over a wide energy range, but overestimate the large angle data at pion energies different from 180 MeV. The two-nucleon force model, on the other hand, tends to underestimate the large angle data. The same is true, to a lesser degree, for smaller angles.

Note that the disagreements of the theoretical predictions with the large angle cross section data must be viewed in a more global context. That is, calculations are usually performed for several observables in the $\pi d \rightarrow \pi d$ channel, and possibly other channels, simultaneously. Successful predictions for some observables can only be obtained at the cost of disagreements elsewhere. Some of these problems were discussed recently by the Lyon[15] and Flinders[16] groups. The Lyon group has studied in detail off-shell effects and the influence of heavy meson exchange. The inclusion of these two effects in their calculation does not significantly affect the predictions for the large angle differential cross sections. The off-shell effects do, however, improve some of their $pp \rightleftarrows \pi d$ predictions. The Flinders group has investigated the sensitivity of their theoretical results to variations in the two-body input. The change of the d-state probability and the contribution of the D_{13} πN amplitude produced little change in the predictions for the differential cross section in the elastic πd scattering.

The most controversial πN input in all calculations for the πNN system is the P_{11} amplitude with its division into a pole and nonpole part which determines the coupling between the NN and the πNN channels. Therefore, one of the first effects the Flinders group studied was that of excluding or including the nonpole part of the P_{11} interaction in those three-body channels that violate the Pauli principle in πd elastic scattering. Excluding the nonpole part reduced the disagreement with the cross sections at large angles at 256 and 325 MeV but at the same time completely spoiled the prediction of the vector polarization iT_{11}. In another series of calculations different P_{11} potentials, all of which reproduced the πN phase shifts below $T_\pi = 400$ MeV equally well, were used. Comparing these predictions for the cross section and vector polarization at $T_\pi = 140$, 256, and 325 MeV, it is clear that it is still not possible to describe the angular and energy dependence of the differential cross section and the vector polarization simultaneously. One of the main conclusions of Ref. 16 was that the tensor polarization T_{20}, at backward angles, for πd elastic scattering, is the observable most sensitive to the choice of the P_{11} interaction; in particular, the way the amplitude is divided into a pole and nonpole part. Therefore, more extensive measurements of this observable than exist presently[36,37] must be the next step to a better understanding of the fundamental πd elastic scattering reaction

ACKNOWLEDGMENTS

This work would have been impossible without the generous help and considerable skills of the staff of SIN. This work was supported by the Bundesministerium für Forschung und Technologie of the Federal Republic of Germany.

[1]A. W. Thomas and R. H. Landau, Phys. Rep. **58**, 121 (1980).
[2]A. Yokosawa, Phys. Rep. **64**, 47 (1980).
[3]For the latest review see A. Švarc, Nucl. Phys. **A434**, 329 (1985); M. P. Locher, SIN Report PR-84-13, Invited talk of the 6th International Symposium on High Energy Spin Physics, Marseille, 1984 (SIN, Villigen, 1984).
[4]C. Fayard, G. H. Lamot, and T. Mizutani, Phys. Rev. Lett. **45**, 524 (1980).
[5]T. Mizutani, C. Fayard, G. H. Lamont, and R. S. Nahabetian, Phys. Lett. **107B**, 177 (1981).
[6]A. S. Rinat, Y. Starkand, and E. Hammel, Nucl. Phys. **A364**, 486 (1981).
[7]A. S. Rinat and Y. Starkand, Nucl. Phys. **A397**, 381 (1983).
[8]I. R. Afnan and B. Blankleider, Phys. Rev. C **22**, 1638 (1980).
[9]B. Blankleider and I. R. Afuan, Phys. Rev. C **24**, 1572 (1981).
[10]H. Garcilazo, Phys. Rev. Lett. **45**, 780 (1980).
[11]R. Händel, M. Dillig, and M. G. Huber, Phys. Lett. **B73**, 4 (1978).
[12]H. G. Hopf, Ph.D. thesis, University of Erlangen, 1983.
[13]M. Betz and T.-S. H. Lee, Phys. Rev. C **23**, 375 (1981).
[14]H. Pöpping, P. U. Sauer, and Zhang Xi-Zhen, *Few Body Problems in Physics,* edited by B. Zeitnitz (Elsevier, New York, 1984), Vol. II, p. 145; H. Pöpping, private communication.
[15]J. L. Perrot, Ph.D. thesis, University of Lyon, 1984; University of Lyon Report LYCEN 8409, 1984.
[16]I. R. Afnan and R. S. McLeod, Phys. Rev. C. **31**, 1821 (1985).
[17]K. Gabathuler *et al.*, Nucl. Phys. **A350**, 253 (1980).
[18]R. C. Minehart *et al.*, Phys. Rev. Lett. **46**, 1185 (1981).
[19]A. V. Kravtsov *et al.*, Nucl. Phys. **A322**, 439 (1979).
[20]R. H. Cole *et al.*, Phys. Rev. C **17**, 681 (1978).
[21]A. Stanovnik *et al.*, Phys. Lett. **B94**, 323 (1980).
[22]R. Keller *et al.*, Phys. Rev. D **11**, 2389 (1975).
[23]M. Akemoto *et al.*, Phys. Rev. Lett. **50**, 400 (1983); M. Akemoto *et al.*, *ibid.* **51**, 1838 (1983).
[24]R. J. Holt *et al.*, Phys. Rev. Lett. **43**, 1229 (1979).
[25]R. Frascaria *et al.*, Phys. Lett. **B91**, 345 (1980).

[26]C. R. Burleson *et al.*, in Book of Abstracts of the Tenth International Conference on Particles and Nuclei, Heidelberg, 1984, edited by T. Güttner, B. Povh, and G. zu Putliz, Vol. I, p. 74.
[27]R. Koch and E. Pietarinen, Nucl. Phys. **A336**, 331 (1980).
[28]M. E. Sadler *et al.*, Phys. Lett. **B119**, 69 (1982).
[29]G. R. Smith *et al.*, Phys. Rev. C **29**, 2206 (1984); G. R. Smith *et al.*, *ibid.* **30**, 980 (1984).
[30]P. B. Bussey *et al.*, Nucl. Phys. **B58**, 363 (1973).
[31]E. L. Mathie *et al.*, Phys. Rev. C **28**, 2558 (1983).
[32]J. C. Alder *et al.*, Phys. Rev. D **27**, 1040 (1983).
[33]See, for example, πN Newsletter, No. 1, January, 1984, edited by G. Höhler and B. M. K. Nefkins.
[34]H. Garcilazo, Phys. Rev. Lett. **53**, 652 (1984); and private communication.
[35]N. Giraud *et al.*, Phys. Rev. C **19**, 465 (1979).
[36]J. Ulbricht *et al.*, Phys. Rev. Lett. **48**, 311 (1982); W. Grüebler *et al.*, *ibid.* **49**, 444 (1982); W. König *et al.*, J. Phys. G **9**, L211 (1983).
[37]R. J. Holt *et al.*, Phys. Rev. Lett. **47**, 472 (1981); E. Ungricht *et al.*, *ibid.* **52**, 333 (1984); E. Ungricht *et al.*, Phys. Rev. C **31**, 934 (1985).